13th IEA Heat Pump Conference
April 26-29, 2021 Jeju, Korea

Numerical analysis of the vortex tube characteristics used within a high temperature heat pump

Constantin Zenz[a,*], Michael Lauermann[a], Mirza Popovac[a]

[a]Austrian Institute of Technology, Giefinggasse 2, 1210 Vienna, Austria

Abstract

The application of heat pumps in high temperature processes bears a high potential with respect to energy savings and reductions of greenhouse gas emissions. As heat pumps operating at high temperatures typically involve high refrigerant pressure levels, followed by high expansion work in the refrigerant cycle, an increase in energy efficiency can be achieved by recovering a part of that expansion energy. This paper investigates the applicability of vortex tubes as expansion devices in heat pumps. A vortex tube separates an incoming high-pressure stream into a cold and hot low-pressure stream, respectively. The flow field characteristics inside a vortex tube are investigated using state-of-the-art CFD tools. Two possible heat pump cycles utilizing a vortex tube are presented and evaluated using a one-dimensional model of a heat pump. It is shown that the applicability of a vortex tube as expansion device in a heat pump is limited due to several restricting factors. One promising configuration and application is identified and presented in detail, where the use of a vortex tube improves the COP by 19% over a standard heat pump.

© HPC2020.
Selection and/or peer-review under responsibility of the organizers of the 13th IEA Heat Pump Conference 2020.

Keywords: Ranque-Hilsch effect; Expansion work; Energy efficiency; CFD; 1D system simulation.

1. Introduction

In standard heat pumps, the expansion process takes place in an isenthalpic throttle valve. Replacing the throttle valve by a so-called Ranque-Hilsch vortex tube has been previously proposed e.g. by Nellis and Klein [1] and Sarkar [2]. A vortex tube, originally invented by Ranque in 1933 [3] and further refined by Hilsch [4], is a simple device with no moving parts, consisting of a tube, where a high-pressure fluid is injected tangentially through nozzles. The fluid develops a swirling flow pattern of high angular velocity, separating the fluid into a stream of high temperature fluid exiting on one axial end near the outer radius of the tube, and a stream of low temperature fluid exiting on the other axial end near the center of the tube. By controlling a valve at the hot end, the fraction of mass flow exiting at the cold side, $\gamma = \dot{m}_c/\dot{m}_i$, called the cold fraction, can be adjusted. In general, if γ increases, T_h increases, and T_c decreases for decreasing γ. At $\gamma = 0.5$, both the hot and cold temperature separation are equal.

Until today, this unique temperature separation effect, called the Ranque-Hilsch effect, is not entirely physically explained, although numerous investigations have been conducted. Hilsch [4] suggested that kinetic energy is transferred from the center to the outer part of the tube through internal friction, with shear work being the underlying mechanism of the temperature separation. Reynolds [5] identified heat and energy fluxes due to turbulent mixing as result of radial pressure and temperature gradients, buoyancy forces and Reynolds shear stresses as underlying physical processes. Ahlborn and Gordon [6] analyzed the vortex tube as a classical refrigeration cycle, identifying a primary loop at the outer radius of the tube as the coolant loop and a secondary

* Corresponding author.
E-mail address: constantin.zenz@ait.ac.at

loop close to the center of the tube as refrigerant loop which performs heat rejection at the outer radius and energy absorption at the center.

Throughout the many investigations that have been conducted both experimentally and numerically on the vortex tube, the working fluid was mostly air. Very little research has been conducted on working fluids other than air. Balmer [7] experimentally analyzed the expansion of liquid water inside a vortex tube, concluding that for inlet pressures of 20 to 50 MPa, a temperature separation of 10 to 20 K is obtainable, notably with both outlet temperatures being higher than the inlet temperature. Although the necessary pressure lies two orders of magnitude above the pressures usually employed in a vortex tube operated with air, Balmer [7] concluded that the working fluid does not necessarily need to be compressible for a temperature separation to occur. Collins and Lovelace [8] performed experiments with two-phase propane inside a vortex tube. This study is especially interesting for the use of vortex tubes in refrigeration cycles, as propane is a common refrigerant and the expansion process in a standard heat pump occurs within the two-phase region. It was concluded in [8] that for inlet vapor qualities above 80%, a significant temperature separation can be obtained, but when the inlet vapor quality is further lowered, the Ranque-Hilsch effect vanishes rapidly.

Based on the research that has been done on the Ranque-Hilsch effect, it does not seem reasonable to replace the throttle valve of a heat pump cycle with a vortex tube, although this has been proposed earlier. The refrigerant entering the throttle valve is usually fully condensed liquid, and pressure levels in heat pumps are by far not sufficient for the Ranque-Hilsch effect to occur with a liquid as working fluid. Also, when two-phase refrigerant enters the vortex tube, e.g. by not fully condensing the fluid, the vapor quality would need to be very high. Therefore, it is concluded that when using a vortex tube inside a heat pump cycle, it must be assured that it is always operated with a fluid in fully gaseous (i.e. superheated) state. This has similarly been concluded previously by Mohiuddin and Elbel [9].

In order to assess different heat pump cycles and analyze possible COP-improvements, a CFD model of the vortex tube has been developed. In this way, the characteristics of the vortex tube under different refrigerants, geometries and operating conditions could be obtained and used for 1D-simulations of different heat pump configurations.

2. CFD Model

The flow inside the vortex tube is modeled as steady, three-dimensional, turbulent and compressible. Therefore, the three-dimensional Favre-averaged Navier-Stokes equations and continuity equation, together with an equation for the conservation of energy are used. The Reynolds stress tensor that comes up when time- (or Favre-) averaging the equations is modeled through the Boussinesq Assumption employing the Standard k-ε turbulence model, which was shown to predict the flow inside a vortex tube with sufficient accuracy, e.g. by Dutta et al. [10]. The model was used with scalable wall functions, making the solver always set $y^* \geq 11.225$ to ensure the first grid point is placed within the fully turbulent sub-layer even if the near-wall mesh is too fine. Viscous heating, i.e. the thermal energy created by viscous shear was included as previous research suggests this mechanism is important in vortex tube flows. Also, a compressibility correction in terms of a dilatation dissipation was included in the k-equation. The density of the fluid was modeled with the ideal gas law, with all material properties being constant except for the specific heat when performing simulations with refrigerants, where c_p was given linear temperature-dependency. To solve this set of equations, a pressure-based coupled solver was used, employing second-order upwind schemes for density, momentum and energy equations, first order upwind schemes for k- and ε-equations, and a second order scheme for pressure. Simulations have also been performed using the third-order MUSCL scheme, but did not show significant changes in the solution, and were therefore omitted for enhancing convergence.

A mesh consisting of tetrahedral cells, with refinements near walls, was used. A purely hexahedral mesh was also created but did not show changes in the solution. Mesh independence was ensured by running numerous simulations with meshes of different cell numbers, using the value of $\Delta T_{h,c} = T_{h,c} - T_i$ for judging mesh independence.

The inlets and outlets were defined as pressure-inlets and pressure-outlets. All walls were treated with a no-slip condition. To judge convergence, besides monitoring the scaled residuals, mass-averaged values of total temperature at both outlets of the vortex tube, T_h and T_c, and the cold fraction, γ, were monitored.

3. Flow pattern

3.1. Air

At first, the geometry used in the study of Skye et al. [11] was used, which is given in Table 1. The exact geometry could not be reproduced, as the dimensions of the hot outlet are unknown, as is the exact geometry of the inlet. The CFD model of [11] was two-dimensional, with a radial exit and a continuous annular inlet, and exhibited discrepancies between experimental and numerical pressure values. Hence also the experimental and CFD results of [11] differ.

Table 1. Vortex tube geometry:

symbol	description	value
L	working length	106 mm
D	tube diameter	11.4 mm
r_c	cold outlet radius	3.1 mm
A_i	total inlet area (6 nozzles)	8.2 mm^2

The working fluid was air, the inlet total pressure was kept at 483 kPa and the inlet total temperature was kept at 294 K. The cold outlet static pressure was kept at ambient pressure and the hot outlet pressure was varied to adjust γ. The results of these simulations are given in Figure 1, where the separation of the hot and cold exit temperatures from the inlet temperature, ΔT_h and ΔT_c, are plotted for varying cold fractions γ. Also, the results of [11] are plotted in Figure 1 for comparison. The obtained results match the CFD results of [11] quite well. It is noted that both the CFD model of this study and that of [11] underpredict the experimental values of ΔT_c. Nevertheless, the qualitative results are identical, exhibiting the same steepness of T-γ-dependency, with $\Delta T_h = \Delta T_c$ at $\gamma \approx 0.5$ and a larger overall temperature separation towards very high values of γ.

Figure 2 shows the profiles of tangential and axial velocity over the radius of the vortex tube at different axial locations. Figure 3 shows the radial profiles of total and static temperature at different axial locations. Both Figures match the velocity- and temperature-profiles produced by Behera et al. [12], suggesting that the physical processes inside the vortex tube are accurately modeled in the underlying CFD-model. In Figure 4, a contour plot of total temperature distribution over the vortex tube is given. Figure 5 shows a contour plot of density.

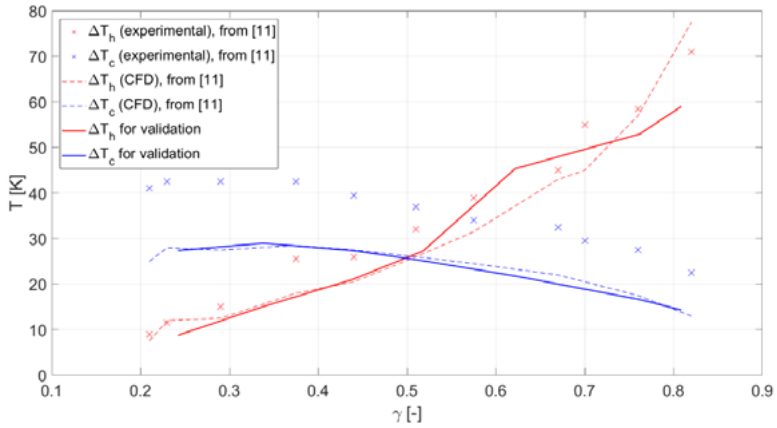

Fig. 1. Total temperature separation at hot and cold outlet as function of γ plotted against CFD and experimental results of [11]

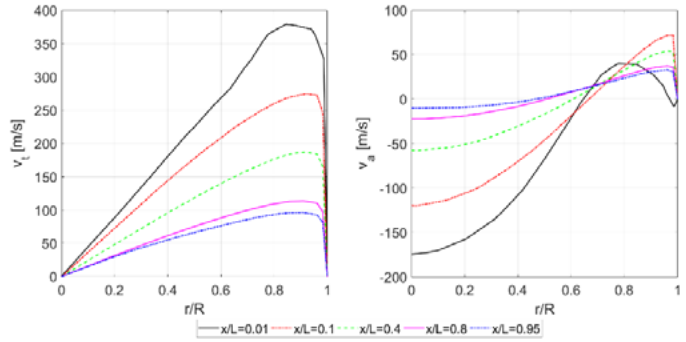

Fig. 2. Tangential (left) and axial (right) velocity profiles at different x/L-locations (air, $\gamma = 0.6$)

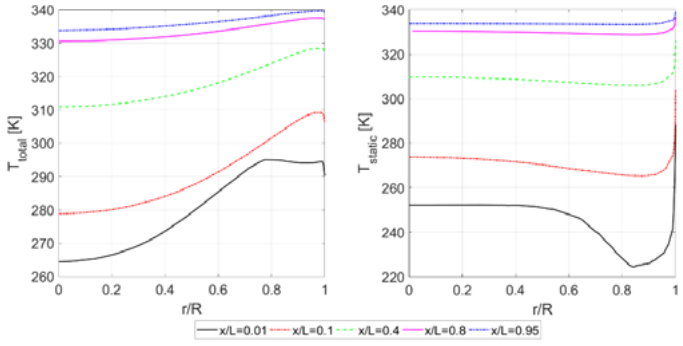

Fig. 3. Total (left) and static (right) temperature profiles at different x/L-locations (air, $\gamma = 0.6$)

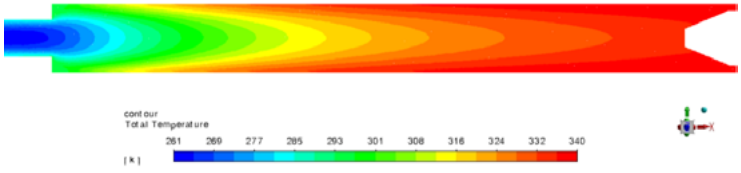

Fig. 4. Contour plot of total temperature throughout the vortex tube (air, $\gamma = 0.6$)

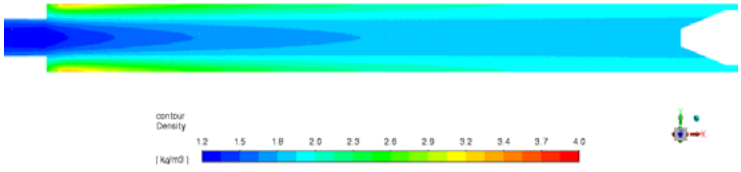

Fig. 5. Contour plot of density throughout the vortex tube (air, $\gamma = 0.6$)

3.2. Water

In order to investigate the flow of an incompressible fluid inside a vortex tube, simulations using liquid water as working fluid have been conducted. The same geometry was used as in the above simulation with air. The geometry is in its overall size comparable to that used by Balmer [7] for experiments with water, although the exact geometric specifications of [7] were not provided. The overall temperature separation obtained for an inlet pressure of 50 MPa was, depending on the cold fraction, around 10 K, with both T_h and T_c being above inlet temperature, which is congruent with the results of [7]. A contour plot of total temperature distribution throughout the vortex tube is provided in Figure 6. It is notable that with water as working fluid, the radial temperature gradient seems to be significantly lower than with air (compared to Figure 5), the temperature variation seems to be almost purely axial. Figure 7 shows tangential and axial velocity profiles and Figure 8 shows total and static temperature profiles at the same axial locations as in the above simulation with air. While the tangential velocity profiles exhibit a similar behavior, the maximum axial velocity at the center is, in contrast to the case with air, not found at $x/L = 0.01$, but at $x/L = 0.1$. Also, the axial velocities at the outer radius exhibit a sharper peak. For the temperature profiles shown in Figure 7 it is notable that while the static temperature profiles seem to be resembling that of the case with air, the total temperature profiles show much less change over the radius compared to Figure 3.

Generally, the flow patterns in terms of velocity and temperature distribution differ from the usual ones observed in vortex tubes operated with gaseous fluids. Another interesting observation is, that when viscous heating is excluded from the CFD model, a lower, yet still significant temperature separation occurs with air. Excluding the viscous heating term from the CFD model for calculations with water, however causes the temperature dissipation to fully vanish, i.e. no temperature gradient over the entire domain of the vortex tube can be observed. This shows that at least in the numerical model, thermal energy created by viscous shear is the only underlying physical process causing the temperature separation. As the results of the numerical analysis deliver similar results to the experimental study of Balmer [7], it is questionable if the Ranque-Hilsch effect is the reason for the temperature separation observed in [7]. The fact that with water both outlet temperatures are higher than the inlet temperature supports the theory that viscous shear is the main reason for this temperature separation.

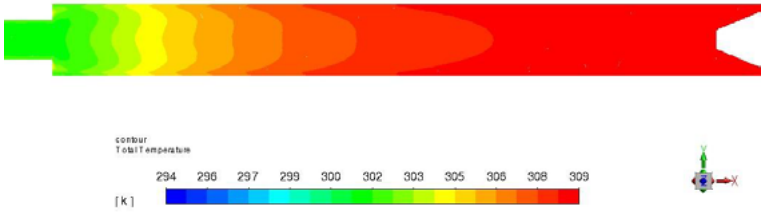

Fig. 6. Contour plot of total temperature throughout the vortex tube (water, $\gamma = 0.54$)

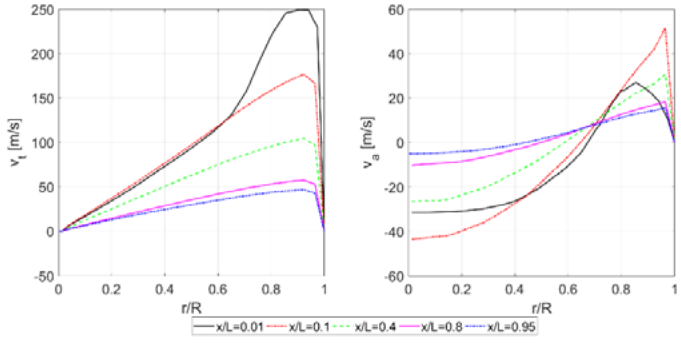

Fig. 7. Tangential (left) and axial (right) velocity profiles at different x/L-locations (water, $\gamma = 0.54$)

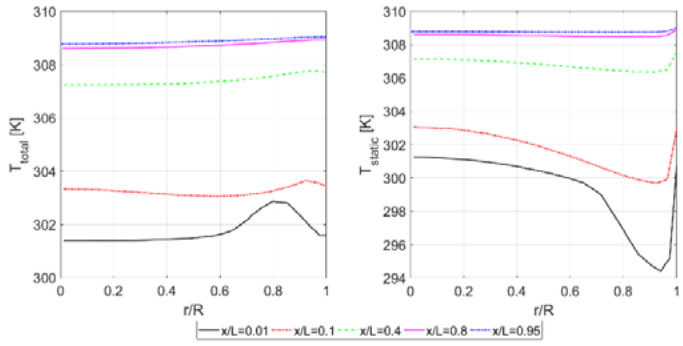

Fig. 8. Total (left) and static (right) temperature profiles at different x/L-locations (water, $\gamma = 0.54$)

3.3. Other Fluids

Simulations with other fluids, mainly natural and synthetic refrigerants, and helium have been conducted. It was noted that in general, the Ranque-Hilsch effect decreases with an increasing molar mass of the fluid. Therefore, helium, being the second lightest element, showed the largest temperature separation. For refrigerants, which generally have a higher molar mass than air, a smaller temperature separation was observed. Using helium as working fluid in a vapor compression cycle is however not feasible as even isentropic compression of helium involves very high temperature rises.

Apart from the molar mass, also thermal conductivity, viscosity and heat capacity ratio of a fluid have been reported to have a significant influence on the Ranque-Hilsch effect [13,14].

As the geometric specifications of the used vortex tube were derived from vortex tubes usually used with air, it is unclear whether a fundamentally different design could substantially improve the Ranque-Hilsch effect when employing a refrigerant. Also, as detailed studies of vortex tubes with refrigerants as working fluids where all geometric specifications and boundary conditions are given were unavailable, a validation of the CFD model for the use of other fluids than air was not possible. Hence, CFD results have to be treated with caution and should merely be used as initial probing to identify possible applications where further experimental investigations seem reasonable.

Figure 9 shows simulation results in terms of hot and cold exit total temperature separation from inlet total temperature for two different vortex tube geometries (different length-to-diameter ratio). The working fluid is R1336MZZ(Z), with an inlet pressure of 10 bar and a cold outlet pressure of 1.978 bar. It can be seen that a change in length-to-diameter ratio has a negligible effect on the temperature separation, and while the pressure ratio between inlet and cold outlet is comparable to that of the case with air (Figure 1), the magnitude of the temperature separation is significantly lower with R1336MZZ(Z) as working fluid.

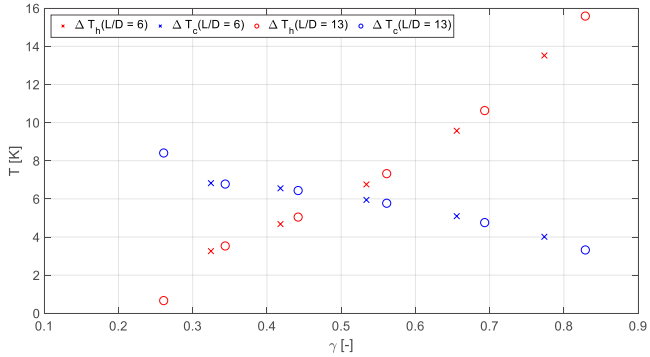

Fig. 9. Total temperature separation at hot and cold outlet as function of γ for two different geometries (R1336MZZ(Z))

4. Applications

Although vortex tubes have been investigated for almost one century by now, and find some specialized applications, there are still no heat pump or refrigeration cycles that make use of the Ranque-Hilsch effect. The focus of this investigation is set on high temperature applications as they are found in industrial steam generation. In Austria, steam generation accounts for 29 % of usable energy in industrial applications, with the majority of that energy being sourced from natural gas, bearing a large potential for the reduction of CO2 emissions [15]. However, to initiate a shift towards the use of (regeneratively sourced) electrical energy for steam generation calls for efficient means of heating. Two possible heat pump cycles for such applications making use of the Ranque-Hilsch effect are presented and discussed here.

4.1. Intermediate Expansion Heat Pump Cycle

When using a vortex tube for expansion in a heat pump cycle, the most promising cycle layout seems to be one introduced similarly by Mohiuddin and Elbel [9]. The schematic layout and log(p)-H-diagram is given in Figure 10. From state 1 to 3, the cycle is identical to that of a conventional heat pump. From state 3 to 4 the refrigerant is expanded to an intermediate pressure level, between that of condenser and evaporator, inside a throttle valve. Then, liquid (5a) and vapor (5b) are separated, with the vapor being fully expanded to evaporator pressure inside a vortex tube (6b/6c). The hot stream (6c) can then be used for further heating purposes, depending on the absolute temperature. The cold stream (6b) is internally recuperated and then mixed with the fully expanded (7a) and evaporated (8) remaining refrigerant.

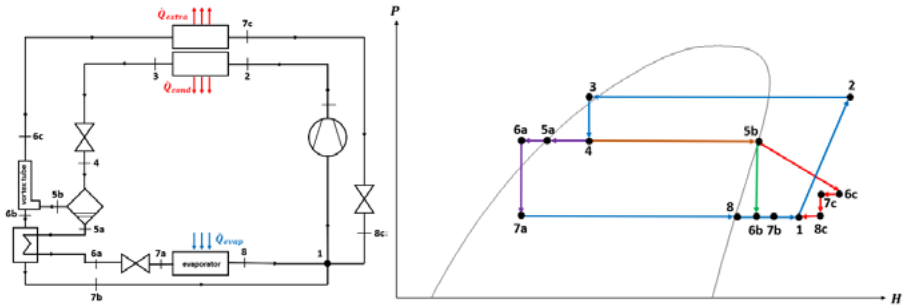

Fig. 10. Schematic cycle layout and theoretical log(p)-H-diagram (based on [9]) of a heat pump with vortex tube expansion

The COP-improvement of such a configuration when compared to a traditional heat pump is estimated by Mohiuddin and Elbel [9] to be around 5 to 10% over a conventional heat pump cycle. Choosing an adequate intermediate pressure level, p_{int}, is crucial for such a configuration, as with p_{int} decreasing, a greater amount of vapor can be utilized inside the vortex tube, but at the same time, the temperature separation effect inside the vortex tube decreases with decreasing inlet pressure. It seems intuitive that there must be an optimum. To estimate the location of this optimum for a given refrigerant, the analytical formulae for calculating the temperature separation inside a vortex tube that were developed by Ahlborn and Gordon [6] were used. These read:

$$\Pi_T = \frac{T_h}{T_c} \approx 1 + \frac{(\kappa-1)\zeta(\gamma+1)}{\kappa} \tag{1}$$

$$\zeta = \frac{p_i - p_c}{p_i + 2p_c} \tag{2}$$

where κ is the heat capacity ratio and p_i and p_c are inlet and cold outlet pressure, respectively. The temperature separation estimated by Eq. (1) is only a very rough estimate, derived using many assumptions, and not taking into account any geometric considerations. Nevertheless, even if the absolute value of Π_T is

far off the reality, its relative change with respect to pressure ratio is believed to show a qualitatively similar behavior to that of a real vortex tube, therefore not influencing the location of that optimum. Using the fact that at $\gamma = 0.5$ the hot and cold temperature separation are equal, absolute temperature values can be obtained:

$$T_h|_{\gamma=0.5} - T_i|_{\gamma=0.5} = T_i|_{\gamma=0.5} - T_c|_{\gamma=0.5} \quad (3)$$

$$T_h|_{\gamma=0.5} = \frac{2T_i|_{\gamma=0.5}}{1+1/\Pi_T} \quad (4)$$

Now, the quantity to be maximized is the difference of enthalpy flow rate between hot and cold outlet, as this quantity includes both the temperature separation, ΔT, that increases with increasing intermediate pressure level and the mass flow rate inside the vortex tube, $\dot{m}$, which decreases with increasing intermediate pressure:

$$\Delta\dot{H} = c_p \dot{m} \Delta T \rightarrow max \quad (5)$$

In Figure 11, $\Delta\dot{H}$ is plotted for a heat pump cycle with R600 as refrigerant, with a condenser pressure $p_{cond} = 26.63$ bar and evaporator pressure $p_{evap} = 6.864$ bar. It can be seen, that there is a clear optimum, below which the inlet pressure of the vortex tube is not high enough, and above which the vapor fraction entering the vortex tube is too low. In this case, the optimum intermediate pressure level is found at $p_{int} = 20$ bar. Any classical heat pump configuration can theoretically be modified in this way. The important question is in each case, if T_h is high enough to be usable with γ being low enough to for the hot end mass flow to be of significant amount.

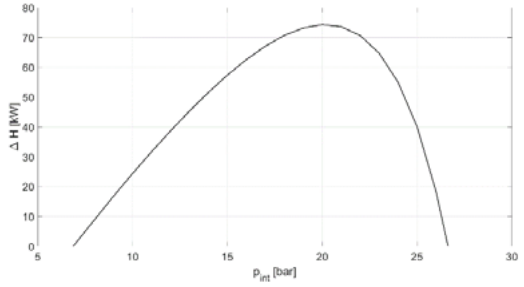

Fig. 11. $\Delta\dot{H}$ as function of p_{int} for R600 in a high temperature heat pump, calculated according to Eqs. (1)-(5)

Apart from maximizing the output of usable energy of the vortex tube itself via Eq. (5), it is at least equally important to tune T_h to a value at which the additional heat provided at the vortex tube's hot exit can be used.

4.2. Heat Boost Cycle

Another way to operate a vortex tube while ensuring the fluid entering the vortex tube remains purely gaseous is a heat boost cycle, which has also previously been suggested by Mohiuddin and Elbel [9]. A schematic layout of such a cycle is given in Figure 12. From state 1 to 2 liquid refrigerant is pumped to a high pressure, where it is then fully evaporated (state 3). From state 3 to 4a/4b, the gaseous refrigerant is expanded inside a vortex tube, using the superheated vapor at state 4a for steam generation.

The advantage of the combined vortex tube heat boost cycle is that the temperature level can be lifted without an increase in pressure. Also, for a given heat source at an already high temperature level, where

otherwise exergetically expensive resistive heating is employed for heat boosting, this configuration seems to be a reasonable alternative. On the other hand, only a small fraction of the overall refrigerant mass flow can be used for steam generation, as high hot end temperatures inside a vortex tube occur at high cold fractions.

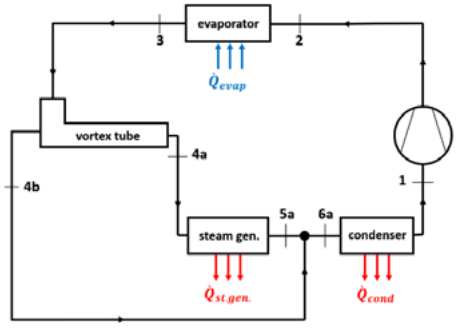

Fig. 12. Schematic cycle layout of a standard vortex tube heat boost cycle with vortex tube

5. Results

A one-dimensional system simulation model for the intermediate expansion cycle (based on the schematic layout presented in Figure 10) was developed as shown in Figure 13. By using the results generated from the CFD model of the vortex tube for different operating conditions and refrigerants to model the vortex tube within these 1D-system simulations, different applications in terms of temperature- and pressure levels, refrigerants and mass flow rates were evaluated. The CFD results of the vortex tube were incorporated in the 1D-model as a lookup-table containing data for several operating conditions. The aim of these system simulations was to identify applications and refrigerants for which the use of vortex tube expansion is promising in terms of COP-improvement.

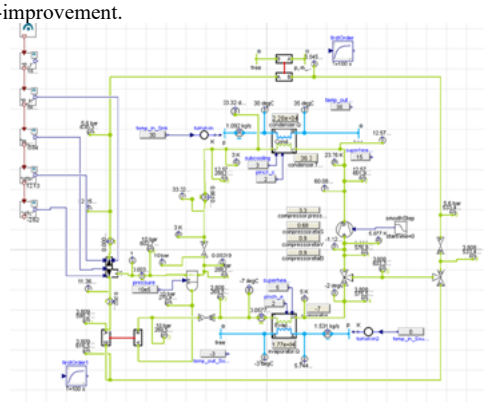

Fig. 13. System simulation model of an intermediate expansion heat pump cycle

As presumed from the findings in Section 4, the intermediate expansion cycle was found to outperform a conventional heat pump cycle in the presence of the following two circumstances:

- A high difference in condenser and evaporator pressure is present, allowing for a relatively low level of intermediate expansion pressure while still maintaining a high enough inlet pressure at the vortex tube.

- The refrigerant exhibits a relatively flat saturation line, yielding a high vapor quality at intermediate expansion pressure level.

Of the conducted simulations, the most promising in terms of COP – improvement was a heat pump cycle aimed at industrial applications where a waste heat source at 70 °C was used to provide heat for steam generation at 160 °C with R1336MZZ(Z) as refrigerant. As a high temperature lift is needed, the difference in condenser and evaporator pressure is high, which in combination with the properties of the refrigerant leads to a significant vapor quality after intermediate expansion. In Figure 14, the log(p)-H-diagrams of both the conventional heat pump cycle and the corresponding intermediate expansion cycle are given, with the hot exit stream of the vortex tube marked in red and the cold exit stream of the vortex tube marked in orange. As can be seen, the separation at intermediate pressure level, combined with the non-isenthalpic expansion in a vortex tube leads to an increased condenser and evaporator heat flow. The COP of the intermediate expansion heat pump cycle was shown to be 19 % higher than that of a conventional heat pump for the same application. The additional heat provided by the hot exhaust of the vortex tube was not used for COP calculations as it is highly case-dependent whether a heat sink exists where this heat can be utilized. Therefore, if demand for additional heat at the temperature level of the vortex tube's hot exit is needed, the COP might increase further.

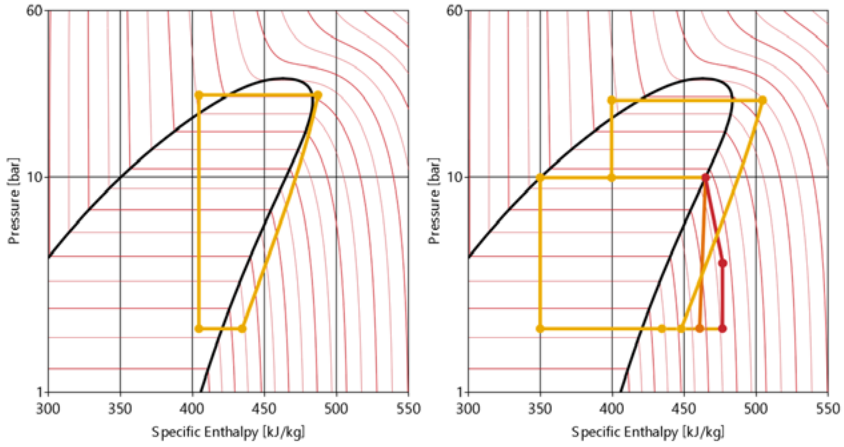

Fig. 14. Log(p)-H-diagrams of conventional (left) and intermediate expansion (right) heat pump cycle for steam generation with R1336MZZ(Z) (result of one-dimensional simulation using results of CFD simulations of a vortex tube)

6. Conclusions

- Although vortex tubes can be operated with liquid working fluids at sufficient inlet pressure, it is not obvious that the underlying physical processes are the same as within vortex tubes operated with gas. The numerical analysis presented here strongly suggests that it is not the same effect that causes energy separation within a vortex tube when operated with liquid as with gas.
- When designing heat pump configurations that involve expansion inside a vortex tube, it is concluded crucial that the fluid remains in gaseous state inside the vortex tube. Two such cycle layouts are presented.
- From the results of CFD simulations it is observed that the Ranque-Hilsch effect decreases when using refrigerants as working fluids. This is believed to partly stem from the higher molecular weight of refrigerants compared to air.
- One of the two presented heat pump configurations, the intermediate expansion heat pump cycle, was simulated and compared to a conventional heat pump cycle. It was found that while for many applications the COP-improvement is negligible, there are cases where vortex tube expansion from an intermediate pressure level can significantly improve the COP. One such cycle aimed at

industrial steam generation using R1336MZZ(Z) as refrigerant is presented and shows a COP improvement of 19 % over a conventional heat pump.
- By identifying promising cases for further investigation using the tools presented in this study - namely a detailed three-dimensional CFD simulation of the vortex tube, combined with a one-dimensional analysis of the heat pump cycle - a foundation for further experimental investigations can be established.

Acknowledgements

The financial support for the work presented in this paper has been provided by FFG – Österreichische Forschungsförderungsgesellschaft mbH (project "VWE", project number 871723).

References

[1] G.F. Nellis & S.A. Klein (2002): The application of vortex tubes to refrigeration cycles. *International Refrigeration and Air Conditioning Conference*, Paper 537.
[2] J. Sarkar (2008): Use of vortex tube as expansion device in isobutane based refrigeration system. *ICRDME*, January 23-25 2008, SUS College of enfineering & Technology Tangori, Mohali (Punjab) India.
[3] G.J. Ranque (1933): Experiments on Expansion in a Vortex with Simultaneous Exhaust of Hot and Cold Air. *Le Journal De Physique et le Radium (Paris)*, Vol. 4, pp. 112-114.
[4] R. Hilsch (1946): Die Expansion von Gasen im Zentrifugalfeld als Kaelteprozess. *Zeitschrift fuer Naturforschung A*, Vol. 1(4), pp. 208-214.
[5] A.J. Reynolds (1961): Energy Flows in a Vortex Tube. *Zeitschrift fuer angewandte Mathematik und Physik ZAMP*, Vol. 12(4), pp. 342-357.
[6] B.K. Ahlborn & J.M. Gordon (2000): The Vortex Tube as Classical Refrigeration Cycle. *Journal of Applied Physics*, Vol. 88(6), pp. 3645-3653.
[7] R.T. Balmer (1988): Pressure-driven Ranque-Hilsch Temperature Separation in Liquids. *Journal of Fluids Engineering*, Vol. 110(2), pp. 161-164.
[8] R.L. Collins & R.B. Lovelace (1979): Experimental Study of Two-Phase Propane Expanded Through the Ranque-Hilsch Tube. *Journal of Heat Transfer*, Vol. 101(2), pp. 300-305.
[9] M. Mohiuddin & S. Elbel (2014): A Fresh Look at Vortex Tubes Used as Expansion Device in Vapor Compression Systems. *International Refrigeration and Air Conditioning Conference*, Paper 1393.
[10] T. Dutta, K.P. Sinhamahapatra, S.S. Bandyopdhyay (2010): Comparison of Different Turbulence Models in Predicting the Temperature Separation in a Ranque-Hilsch Vortex Tube. *International Journal of Refrigeration*, Vol. 33(4), pp. 783-792.
[11] H.M. Skye, G.F. Nellis, S.A. Klein (2006): Comparison of CFD Analysis to Empirical Data in a Commercial Vortex Tube. *International Journal of Refrigeration*, Vol. 29(1), pp. 71-80.
[12] U. Behera, P.J. Paul & S. Jacob (2008): Numerical Investigations on Flow Behaviour and Energy Separation in Ranque-Hilsch Votex Tube. *International Journal of Heat and Mass Transfer*, Vol. 51(25), pp. 6077-6089.
[13] N. Li, Z. Wang, X. Han, G. Chen (2014): Experimental Study of the Coupling Characteristics Between Vortex Tube and Refrigerants. *International Refrigeration and Air Conditioning Conference*, Paper 1518.
[14] X. Han, N. Li, K. Wu, Z. Wang, L. Tang, G. Chen, X. Xu (2013): The Influence of Working Gas Characteristics on Energy Separation of Vortex Tube. *Applied Thermal Engineering*, Vol. 61, pp. 171-177.
[15] Statistik Austria. *Nutzenergieanalyse Oesterreich 2017*. URL: http://www.statistik.at/web_de/statistiken/energie_umwelt_innovation_mobilitaet/energie_und_umwelt/energie/nutzenergieanalyse/index.html (accessed: 14.11.2019).